THE JOURNAL OF BIOLOGICAL CHEMISTRY
Vol. 277, No. 16, Issue of April 19, pp. 13724–13731, 2002
© 2002 by The American Society for Biochemistry and Molecular Biology, Inc.
Printed in U.S.A.

Allosteric Communication between Signal Peptides and the SecA Protein DEAD Motor ATPase Domain*

Received for publication, January 3, 2002, and in revised form, January 30, 2002
Published, JBC Papers in Press, February 1, 2002, DOI 10.1074/jbc.M200047200

Catherine Baud, Spyridoula Karamanou, Giorgos Sianidis, Eleftheria Vrontou, Anastasia S. Politou‡, and Anastassios Economou§

From the Institute of Molecular Biology and Biotechnology, Foundation of Research and Technology-Hellas and Department of Biology, University of Crete, P.O. Box 1527, GR-711 10 Iraklio, Crete, Greece and the ‡Department of Biological Chemistry, Medical School, University of Ioaninna, GR-45110 Ioannina, Greece

SecA, the preprotein translocase ATPase is built of an amino-terminal DEAD helicase motor domain bound to a regulatory C-domain. SecA recognizes mature and signal peptide preprotein regions. We now demonstrate that the amino-terminal 263 residues of the ATPase subdomain of the DEAD motor are necessary and sufficient for high affinity signal peptide binding. Binding is abrogated by deletion of residues 219–244 that lie within SSD, a novel substrate specificity element of the ATPase subdomain. SSD is essential for protein translocation, is unique to SecA, and is absent from other DEAD proteins. Signal peptide binding to the DEAD motor is controlled in *trans* by the C-terminal intramolecular regulator of ATPase (IRA1) switch. IRA1 mutations that activate the DEAD motor ATPase also enhance signal peptide affinity. This mechanism coordinates signal peptide binding with ATPase activation. Signal peptide binding causes widespread conformational changes to the ATPase subdomain and inhibits the DEAD motor ATPase. This involves an allosteric mechanism, since binding occurs at sites that are distinct from the catalytic ATPase determinants. Our data reveal the physical determinants and sophisticated intramolecular regulation that allow signal peptides to act as allosteric effectors of the SecA motor.

Several cellular polypeptides cross biological membranes prior to acquiring their native state. Such proteins are delivered by chaperone-like factors (*e.g.* signal recognition particle and SecB) (1, 2) to membranes and subsequently cross them through specialized pumps termed preprotein translocases or translocons (3–5). The bacterial Sec translocase comprises the membrane proteins SecYEGDFYajC and the peripheral ATPase SecA (4, 5). Several of these components are essential and conserved in the three domains of life. Secretory proteins bind to the SecA motor and activate its ATPase. This triggers SecA "insertion-deinsertion" cycles at SecYEG (6, 7), allowing processive translocase movement along the polymeric substrate (8) in defined steps (9, 10). Substrates are thought to transverse the bilayer through a putative "pore" formed by the essential SecYEA core (11–13). Proton motive force (14), SecG (15, 16), and SecDF (8, 16) regulate SecA cycling.

* This work was supported by European Union Grants ERBFMRXCT-960035, QLK3-CT-2000-00082, QLRT-2000-00122, and RTN1-1999-00149 (to A. E.) and Pfizer, Inc. (to A. E.). The costs of publication of this article were defrayed in part by the payment of page charges. This article must therefore be hereby marked "*advertisement*" in accordance with 18 U.S.C. Section 1734 solely to indicate this fact.

§ To whom correspondence should be addressed. Fax/Tel.: 30-81-391166; E-mail: aeconomo@imbb.forth.gr.

Dimeric SecA is built of defined mechanical parts (17, 18). Each protomer (102 kDa) comprises a 68-kDa N-terminal domain (N68) homologous to ATPase motor domains of DEAD helicases (8, 18, 19) and a C-terminal (C34) dimerization domain (17, 20). The SecA DEAD motor forms a proposed mononucleotide binding fold (18, 21) built from an amino-terminal region harboring a nucleotide binding subdomain (NBD) that contains Walker box A and B sequences (DEAD helicase motifs I and II; Fig. 2*A*) (22) and the intramolecular regulator of ATP hydrolysis (IRA2) subdomain (18). N68 displays a high, unregulated ATPase activity (17).

Deletion and point mutants helped determine the basic features of SecA catalysis (17, 18). IRA1, an essentiaI molecular switch in C34, regulates the DEAD motor ATPase through C34/DEAD motor binding (17). SecA ATPase is thus activated only under appropriate conditions (*i.e.* by substrates at SecYEG) and not in vain (*i.e.* in the cytoplasm).

An important unresolved question is the molecular mechanism of SecA/preprotein interaction and how this regulates the DEAD motor. Several assays have demonstrated that signal peptides and whole preproteins bind to soluble SecA and alter its conformation (23–28). Signal peptides activate SecA lipid ATPase with (29) or without (24, 26) the simultaneous addition of corresponding mature regions. On the other hand, nucleotides alter the efficiency of SecA/preprotein cross-linking (26, 30). Finally, a full-length preprotein has been cross-linked to residues 267–340 of SecA (31). However, whether this region represents a binding site for either the signal peptide or the mature region or whether cross-linking resulted from spatial proximity at a site distinct from the binding site proper was not determined.

To determine the molecular features of SecA/preprotein interaction, we localized and quantitated signal peptide binding onto SecA. We found that the signal peptide binds on the amino-terminal ATPase subdomain of the DEAD motor, at a site distinct from the catalytic determinants. Binding requires SSD, a novel substrate specificity domain that is essential for protein translocation. Signal peptide binding affects conformation of the ATPase subdomain and leads to DEAD motor ATPase repression. Signal peptide binding to soluble SecA is, like ATP hydrolysis (17), repressed by IRA1. These interactions dictate an ordered cascade leading to allosteric activation of translocase by signal peptides.

EXPERIMENTAL PROCEDURES

Bacterial Strains and Recombinant DNA Experiments—Strains and DNA manipulations were as described (17, 32).

Histidine-tagged N68 Fragments—pIMBB192 (His_6N1–227), pIMBB194 (His_6N1–234), pIMBB88 (His_6N1–349), and pIMBB134 (His_6N1–420) were constructed by PCR from pIMBB7, using as forward primer X80 (5′-GGCCCGTACATATGCATCACCATCACCATCAC-3′)

This paper is available on line at http://www.jbc.org

and reverse primers X139 (5′-CGCGACGGATCCGCCGGAAATGATCAGCGG-3′) for N1–227, X140 (5′-CGCGACGGATCCTTCCGAGCTGTCTTCTGC-3′) for N1–234, X83 (5′-CGCGACGGATCCCCAGCGACGGCCCTGCATGG-3′) for N1–349, and X121 (5′-CGCGACGGATCCAATCATTGGACGGTTGGTCGG-3′) for N1–419. Gel-purified products digested with *Nde*I and *Bam*HI were inserted in pET3a.

pIMBB94 (N335–610His_{10}) was constructed by PCR from pIMBB7 using forward primer X90 (5′-GGCCCGTACATATGATCGTTGACGAACACACC-3′) and reverse primer X87 (5′-CCGGACCTCGAGCAGTTTACGCATCATGCC-3′). Gel-purified product digested with *Nde*I and *Xho*I was inserted in pET22b.

pIMBB146 (N420–610His_{10}) was constructed from pIMBB7 using forward primer X122 (5′-GGCCCGTACATATGCGTAAAGATCTGCCGGACCTG-3′) and reverse primer X123 (5′-CGCGACGGATCCCAGTTTACGCATCATGCCGG-3′). Gel-purified product digested with *Nde*I/*Bam*HI was inserted in pET16b.

pIMBB98 (N244–478His_{10}) was constructed by PCR from pIMBB7, using forward primer X94 (5′-GGCCCGTACATATGCCGCACCTGATCCGTCAG-3′) and reverse primer X95 (5′-CGGGACCTCGAGCAGGACGTTGTGCTTAATAC-3′). Gel-purified product digested with *Nde*I and *Xho*I was inserted in pET22b.

pIMBB117 (His_6SecAΔ219–240) was generated upon replacement of the 2.5-kb *Nco*I fragment of pIMBB7 (His_6SecA) (18) with the corresponding fragment from pGJ1 (SecAΔ219–240) (33). pIMBB120 (His_6N68Δ219–240) was generated by subcloning the 2.6-kb *Bam*HI/*Kpn*I fragment of pIMBB117 to corresponding sites of pIMBB8 (His_6N68) (17).

Chemicals and Biochemicals—Proteases, inhibitor pefabloc (4-(2-aminoethyl)-benzenesulfonyl fluoride), and nucleotides were from Roche Molecular Biochemicals. *E. coli* phospholipids were from Avanti Polar lipids. Sequenase, [^{35}S]methionine (1000 Ci/mmol), and [γ-^{32}P]ATP (5000 Ci/mmol) were from Amersham Biosciences. [^{3}H]Acetic anhydride (100 mCi/mol) was from ICN. Me_2SO, acetonitrile, and trifluoroacetic acid (HPLC grade) were from Merck. DNA enzymes were from MINOTECH, cloning vectors were from Invitrogen, and oligonucleotides were from MWG. Dithiobis(succinimidyl propionate) was from Pierce. All other chemicals were from Sigma.

Protein and Peptide Purification, Labeling, and Immobilization—Sec proteins, His-tagged derivatives, and translocation substrates were purified as described (17, 18, 29).

High Performance Liquid Chromatography—Tryptic peptides (200 μg of total protein/run) were injected onto a reverse phase column (UP5WRP-25; Interchrom) in a Shimadzu LC-10A_{VP} HPLC instrument equipped with a diode array detector and CLASS-VP 5.0 software. Peptides were eluted (50-min run at 0.75 ml/min) with a gradient of 25–56% (v/v) acetonitrile in 0.1% (v/v) trifluoroacetic acid. Elution was monitored at 220 nm. Fractions (0.75 ml) were dried (SpeedVac; Savant) and resolubilized in Laemmli sample buffer. Proteins were separated by electrophoresis on high Tris (hT) (34) gels and either visualized by silver staining or electrotransferred (4 °C, 200 mA; 90 min) to polyvinylidene difluoride membrane (Immobilon P; Millipore Corp.). Following Coomassie Blue staining, peptides were subjected to Edman degradation (Alba Biosciences, Birmingham, UK).

Signal Peptide Synthesis—3K7L (MKQKKLALLLALLLASSSASAC) and 1K2L (MKQQQAALAAAAALASSSASAC) prepared by standard Fmoc (*N*-(9-fluorenyl)methoxycarbonyl) solid phase synthesis were purified by HPLC on a semipreparative resin (C18-SynChropak RP-P.250 × 7.8; Synchrom) and were handled and stored as described (24, 35). Purified peptides dissolved in Me_2SO (~5 mg/ml) were stored at −80 °C.

Peptide Labeling—Peptides were labeled by ^{3}H acetylation of the N-terminal group (36) and stored at −20 °C. The functional state of [^{3}H]3K7L was tested by comparing its N68 ATPase inhibition activity with that of unlabeled 3K7L.

Affinity Resin—3K7L was immobilized on CNBr-activated Sepharose 4B (Amersham Biosciences). 3K7L (2 mg/ml resin in 0.1 M $NaHCO_3$, pH 8.3, 0.5 M NaCl) was coupled onto the matrix at 4 °C. Excess ligand was washed away, and the remaining active groups were blocked with 0.1 M Tris·Cl, pH 8 (2 h).

Cross-linking and Proteolytic Digestion—[^{3}H]3K7L (1500 pmol; 55,000 cpm) was incubated (40-μl reactions; 5 min at 4 °C) with SecA or derivatives (150 pmol in buffer H (50 mM Hepes, pH 8, 50 mM KCl, 5 mM $MgCl_2$, dithiothreitol prior to incubation with dithiobis(succinimidyl propionate) (10-fold molar excess; 20 min; 0 °C). After a 15-min incubation on ice, the reactions were quenched with 125 mM Tris-HCl, pH 7.9. Cross-linking was visualized developed by fluorography (Amplify) and quantitated by phosphorimaging (TR screens/ImageQuant software; Molecular Dynamics, Inc., Sunnyvale, CA).

Proteolytic digests (50-μl final volume in buffer B) contained 20 pmol of proteins and a 15-fold (N1–349) or 20-fold (SecA and N68) molar excess of signal peptide. After a 5-min incubation on ice, trypsin (25 μg/ml) was added for an additional 45 min, and the reaction was stopped with pefabloc (10 mM). Samples were then analyzed by HPLC and SDS-PAGE (10% hT gels) and visualized by silver staining.

Surface Plasmon Resonance—Optical biosensor measurements were on an IBIS II instrument (Echochemie). 3K7L (3 μg in 50 μl from a 60 μg/ml stock in 10 mM Hepes, pH 8.5) was added onto carboxymethylated dextran-coated gold sensor disks (CMD6 or CMD20; Xantec) and was cross-linked via NH_2-specific *N*-ethyl-*N*′-(dimethylaminopropyl)carbodiimide)/*N*-hydroxysuccinimide. The surface was equilibrated with buffer H and regenerated with 100 mM HCl. Data were collected for 750 s and were analyzed using IBIS Kinetic Analysis software. The association constant (K_a) was determined from data points of a range of protein concentrations at equilibrium (steady state of the association phase) by linear regression using the integrated rate method (37).

Preparation of α-SSD Monospecific Antibodies—α-244–385 antibodies were purified from α-N244–478 serum. N385–610 was immobilized on CNBr-Sepharose (5 mg/ml gel, 12 h, 4 °C). Remaining active groups were blocked with 0.1 M Tris-HCl, pH 8. The α-244–478 serum was then adsorbed on the resin (1 h, 22 °C) to remove 385–478 interacting antibodies. Flow-through material was collected and tested for specificity by Western blot and immunoblotting.

Miscellanous Techniques—Protein concentration determination, *in vitro* translocation assays, enzyme kinetics, CD spectroscopy, and protein electrophoresis were as described (7, 17, 18).

RESULTS

Functional Signal Peptides Bind to the DEAD Motor Domain of SecA—To identify the signal peptide binding region of SecA, we used 3K7L, a chemically synthesized signal peptide that binds soluble SecA and promotes efficient protein secretion *in vivo* (24, 26). The peptide we synthesized has all of the functional features described previously; it activates SecA lipid ATPase (Fig. 1*A*) and inhibits translocation ATPase activity while leaving basal and membrane ATPase activities largely unaffected. In support of previous data (24), none of these effects are observed with 1K2L, a nonfunctional signal peptide (not shown). Furthermore, 3K7L competitively inhibits translocation of a full-length preprotein such as proOmpA into inverted inner membrane vesicles when added prior (*B*, *lane 4*) but not after (*lane 5*) initiation of the reaction.

To determine which SecA primary domain is responsible for 3K7L binding, we employed chemical cross-linking (Fig. 1*C*). Mixtures of tritiated 3K7L (*lane 1*; see "Experimental Procedures") with SecA or N68 or C34 (17, 18) were cross-linked with dithiobis(succinimidyl propionate). Under nonreducing conditions, [^{3}H]3K7L co-migrates with SecA (*lane 3*) or N68 (*lane 6*) but not with C34 (*lane 9*). Cross-linking of [^{3}H]3K7L was more intense with N68 than with SecA (see also below), was extensively reduced by dithiothreitol (*DTT*; *lanes 4* and *7*), and could be competed by the addition of an excess of nonlabeled 3K7L (*lanes 5* and *8*). No cross-linking of [^{3}H]3K7L was observed to a BSA control (*lane 2*). These results indicated that signal peptides bind on the SecA DEAD motor. To further test this possibility, SecA and N68 were passed over agarose-immobilized 3K7L (see "Experimental Procedures"). Both proteins were retained on the affinity matrix (Fig. 1, *D* and *E*; *lanes 1–3*) and were competitively eluted by an excess of free 3K7L (*lane 4*). BSA did not bind to the matrix and was recovered in the flow-through (*F*, *lane 2*).

We conclude that signal peptides bind on the SecA DEAD motor (N68 domain).

Residues 1–263 Contain a Fully Functional Signal Peptide Binding Site—To identify the DEAD motor subdomain responsible for signal peptide binding, N68 was trypsinized to large peptides that were amino-terminally sequenced (Fig. 1*G*; *lane 2*; p36, p35, p25, p24, p16, and p12). Binding of these peptides to the 3K7L affinity matrix was tested. The amino-terminal p36 and p35 fragments were quantitatively retained on the matrix, since they were not present in the flow-through (*lane*

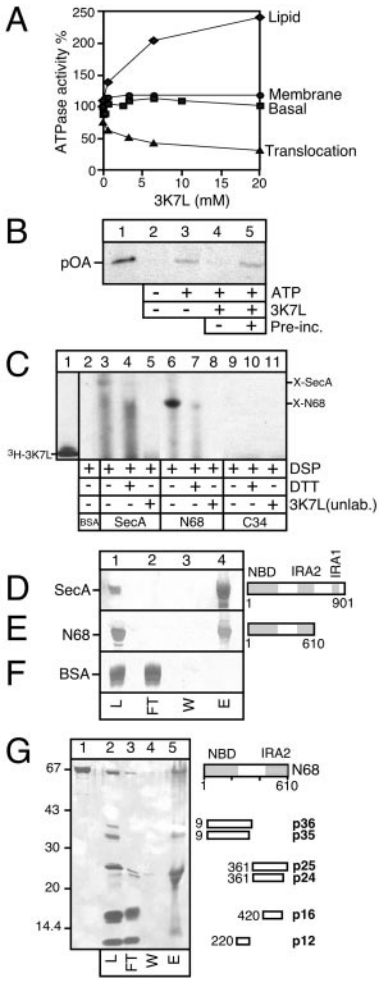

FIG. 1. **The synthetic signal peptide (3K7L) is functional and binds to the N-domain of SecA.** *A*, the effect of 3K7L on ATP hydrolysis by SecA (20 μg/ml; 50-μl reactions) was followed by measuring release of inorganic phosphate (29). Basal activity was measured in buffer B (50 mM Tris-Cl, pH 8.0, 1 mM dithiothreitol, 0.4 mg/ml BSA) supplemented with ATP (1 mM). For the other activities (as defined by Lill *et al.* (29) and Brundage *et al.* (53)), the following additions were made: liposomes (300 μg/ml; lipid ATPase); SecYEG proteoliposomes (300 μg/ml; membrane ATPase); and SecYEG proteoliposomes plus proOmpA (*pOA*; 30 μg/ml; translocation ATPase) as indicated. Reactants were mixed at 4 °C and incubated (30 min; 37 °C) with the indicated 3K7L amounts. ATPase activities are expressed as a percentage of the activity of a corresponding control reaction containing no 3K7L peptide. *B*, signal peptide competes proOmpA for translocation. *In vitro* translocation reactions (30 min, 37 °C) were performed in buffer B containing SecA (30 μg/ml), SecYEG proteoliposomes (250 μg/ml) in the presence of ^{35}S-proOmpA (50,000 cpm; marked *pOA*), and, when indicated, ATP (1 mM) and 3K7L (40 μg/ml). In *lane 5*, the signal peptide was added 10 min after translocation of ^{35}S-proOmpA was initiated (marked *preinc.*). Samples were digested with proteinase K (1 mg/ml, 15 min, 4 °C). The protease-protected ^{35}S-proOmpA was detected on a SDS-polyacrylamide gel (15%) by fluorography. *C*, signal peptide chemical cross-linking. SecA and N68 (100 pmol) in buffer H were incubated (5 min; 4 °C) with a 15-fold molar excess of [^{3}H]3K7L prior to the addition of dithiobis(succinimidyl propionate) (see "Experimental Procedures"). Samples were analyzed on hT gels (16% acrylamide (*lane 1*) or 10% acrylamide (*lanes 2–11*)) in the absence or presence of dithiothreitol as indicated, followed by autoradiography. *X-SecA* and *X-N68*, cross-linked species. *3K7L (unlab.)*, 20-fold excess of unlabeled signal peptide. *D–F*, signal peptide affinity chromatography. SecA or N68 or BSA (0.5 mg in buffer B) were loaded (0.25 ml/min) onto an affinity matrix (150-μl bed volume) comprising 3K7L immobilized on cyanogen bromide-activated Sepharose (*lane 2*) and incubated for 15 min (4 °C). After extensive wash with buffer B, bound proteins (*D* and *E*) were competitively eluted with 3K7L (0.5 mg/ml), trichloroacetic acid-precipitated, separated in 10% hT gels, and visualized by silver staining. *L*, loading; *FT*, flow-through; *W*, wash; *E*, elution. *G*, signal peptide affinity chromatography of N68 tryptic fragments. N68 (250 μg in buffer B, *lane 1*) was digested with trypsin (25 μg/ml; 45 min, 4 °C) to generate the indicated proteolytic fragments. The reaction was terminated by pefabloc (10 mM). Peptides were identified by N-terminal sequencing and calculation of C termini from the molecular weight as follows: p36 (^{9}VFGSRND . . . ^{360}), p35 (^{9}VFGSRND . . . ^{338}), p25 (^{361}EGVQIQN . . . ^{586}), p24 (^{361}EGVQIQN . . . ^{576}), p16 (^{420}RKDLPLV . . . ^{560}), p12 (^{220}TPLIISG . . . ^{329}). Tryptic peptides (loading material (*L*)) were assayed for 3K7L binding as in *D–F*. Chromatography fractions resolved on a 10% hT gel were visualized by silver staining. *FT*, flow-through; *W*, wash; *El*, elution. The molecular masses (kDa) of marker proteins are indicated.

3). p16 (contains IRA2) (18) and p12 were recovered in the flow-through (*lane 3*), suggesting that these regions do not contain a fully functional signal peptide binding site. p25 and p24 (containing IRA2 and upstream sequences) were largely retained on the matrix (*lane 5*), suggesting that they either bind signal peptide directly or that they coelute with amino-terminal fragments (such as p35 and p36) due to the tight association of the ATPase subdomain with IRA2 (18).

To unambiguously delimit the signal peptide binding determinants, we generated truncated recombinant N68 derivatives synthesized with oligohistidinyl extensions (Fig. 2*A* and Ref. 18). Purified recombinant fragments (Fig. 2*B*) were shown by far UV sprectropolarimetry to be folded (data not shown and Ref. 18).

Binding of [^{3}H]3K7L to N68 fragments was examined by cross-linking (Fig. 2*C*). Cross-linking to N1–263, N1–349, and N1–479 (Fig. 2*C*, *lanes 5–7*) and N1–420 (data not shown) was at least as strong as that of SecA and N68 (*lanes 1* and *2*). Interestingly, reduced but measurable cross-linking was also obtained with N1–234 (*lane 4*), while cross-linking to the slightly smaller N1–227 fragment was weak (*lane 3*). To exclude artifacts due to truncated constructs, in the same assay we tested a full-length SecA with an internal deletion of residues 219–240 (33). SecAΔ219–240 is dominant negative *in vivo* (33), has no detectable structural defects since it is proteolytically stable (Fig. 2*B*, *lane 14*) (33), and displays wild type basal ATPase (K_{cat} = ~4 min^{-1}). No detectable cross-linking was obtained with either SecAΔ219–240 (Fig. 2*C*, *lane 14*) or N68Δ219–240 (*lane 15*). Similarly, little or no cross-linking was obtained with fragments that did not contain the 1–270 sequence (*lanes 8–12*) or with a control protein (*lane 13*).

To further test and quantitate 3K7L association to SecA and derivatives with a direct method that eliminates potential aggregation artifacts, we developed a 3K7L optical biosensor (Fig. 2*E*; see "Experimental Procedures"). N68 binding (*lane 2*) to 3K7L is higher than that of SecA (*lane 1*). In agreement with the cross-linking results, N1–234, N1–263, N1–349, and N1–479 (*lanes 4–7*) bind to 3K7L as well as or even more strongly than SecA, whereas N1–227 (*lane 3*) binds poorly. Fragments devoid of amino-terminal sequences (*lanes 8–12*), control proteins (*lane 13*), SecAΔ219–240 (*lane 14*), and N68Δ219–240 (*lane 15*) show little or no detectable binding.

These data can be rationalized by kinetic analysis (Table I). The binding affinity (K_D) of SecA for 3K7L is almost 3 times reduced when compared with that of N68, indicating that N68 is somehow activated for binding (see below). N1–263 has similar affinity to N68, whereas that of N1–234 is high but ~3-fold reduced compared with that of N68. In contrast, the affinity of N1–227 is drastically reduced (~15-fold), suggesting that it is missing either residues important for efficient 3K7L binding or local structural features.

We conclude that N1–263 contains a fully functional signal peptide binding site. Since the mutated proteins show no structural defect, our data suggest that residues 219–244 are essential for signal peptide binding to an unknown region of 1–263, whereas residues 234–263 may optimize the binding reaction.

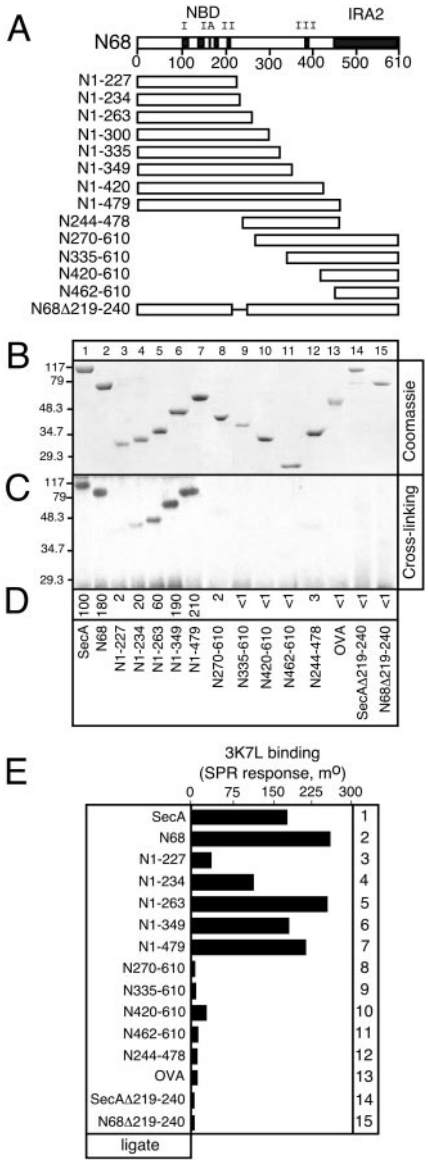

FIG. 2. **Binding of N68 truncations to 3K7L.** *A*, schematic representation of N68 truncations. *Latin numerals* indicate DEAD helicase superfamily 2 motifs. *Numbers* in the name of each fragment represent the first and the last amino acid of the sequence. *B–D*, cross-linking of [^{3}H]3K7L to SecA and truncations. Purified N68 truncations (5 μg) were resolved on a 10% hT gel and visualized by Coomassie staining (*A*). *C*, an identical set of polypeptides (150 pmol in buffer H) were cross-linked with [^{3}H]3K7L and analyzed as in Fig. 1*C*. Positions of molecular mass standards (kDa) are indicated. Cross-linking (expressed as a percentage of that of SecA) was quantitated by phosphorimaging (*D*). *E*, binding of SecA and derivative fragments to a signal peptide optical biosensor. Polypeptides (1 μM in buffer H) were added to 3K7L immobilized on a biosensor chip (see "Experimental Procedures"). The change in refractive index was followed with time, and the binding response at equilibrium (t = 750 s; expressed in millidegrees) is shown.

Structure of the Amino-terminal ATPase Region of SecA—To characterize folding and subdomain structure of the DEAD motor amino-terminal region that contains the ATPase and signal peptide binding determinants (Fig. 2), we combined two approaches: (*a*) limited trypsinolysis of amino-terminal N68 fragments (Fig. 3*A*) and (*b*) comparison of SecA amino-terminal sequences with those of DEAD helicases of known three-dimensional structure (Fig. 3*B*). The N1–420 construct is colinear with the most prominent proteolytic fragment of 46 kDa derived from SecA and N68 (17, 18) or from N1–479 (Fig. 3*A*, *lanes 15–16*, *open arrow*) and retains protease resistance when synthesized as an independent polypeptide (*lanes 13* and *14*).

TABLE I
Kinetic parameters of signal peptide binding to SecA and derivative domains

A range of protein concentrations ensuring binding saturation (0.05–10 μM) were added to 3K7L immobilized on a biosensor (see "Experimental Procedures"). n, number of repeats of the measurement.

Protein	$K_{D,\ 3K7L}$	n
	μM	
SecA	3.16	5
N68	1.36	4
N1–227	21	4
N1–234	4.9	2
N1–263	1.8	3
SecAΔIRA1-(783–795)	1.23	3
SecAW775A	1.4	3

N1–420 contains DEAD superfamily 2 motifs I–III (21, 22), and its predicted secondary structure aligns well with that of other DEAD proteins such as UvrB (Fig. 3*B*). Taken together, these observations suggest that, as in all corresponding DEAD helicase domains, N1–420 forms a single structural unit (Fig. 3*B*).

All trypsinized truncation fragments give rise to a proteolytic peptide of the size of N1–227 (~26 kDa; Fig. 3*A*, *even lanes*, *filled arrow*). Since all of these recombinant polypeptides display similar ATPase activity with the previously characterized minimal ATPase domain N1–263 (K_{cat} = ~0.05–0.1 min^{-1} (18)), N1–227 must represent the minimal catalytic and structural ATPase core within N1–263 and N1–420 (18).

A striking feature of N1–420 is a large insertion (residues ~220–360) bracketed by DEAD motifs II and III (Fig. 3*B*). This region is absent from other DEAD proteins and encompasses residues 227–263 essential for signal peptide binding (Fig. 2). The 220–360 region is predicted to be structured (40% α-helix, 17% β-sheet). Interestingly, the 220 and 360 boundaries can be proteolytically dissected (Fig. 1*G*), and a stable p12 tryptic peptide that spans most of it can be identified (Fig. 1*G*). These data suggest that the 220–360 region forms a distinct structured element within N1–420. This region of SecA is similar to nonhomologous "substrate specificity domains" that are widespread appendages of DEAD proteins (*e.g.* in UvrB residues 89–117, 148–322, and 347–376; Fig. 3*B*; see "Discussion") and that provide specialization of DEAD motors for their respective substrates (38, 39). We therefore term the 220–360 element in SecA the SSD (substrate specificity domain).

Importantly, SecAΔ219–240, which carries a small deletion in SSD, is defective in signal peptide binding (Fig. 2) and catalyzes no detectable protein translocation (Fig. 2*C*, *lane 6*) in a standard *in vitro* assay (9). In contrast, SecA catalyzes proOmpA translocation into SecYEG proteoliposomes (*lane 3*), where proOmpA becomes protease-accessible only upon solubilization of the membrane with detergent (*lane 4*).

We conclude that the amino-terminal ATPase subdomain and the adjacent substrate specificity domain are integral parts of the structured N1–420 domain. SSD is a novel essential determinant of translocase catalysis.

Signal Peptide Binding Causes Conformational Changes to N1–420—To test if 3K7L affects conformation of the DEAD motor, we used limited trypsinolysis (Fig. 4*A*). N1–349 digestion in the absence of 3K7L (*lane 8*) leads to formation of two prominent low molecular weight peptides (p12, p4) of 12 and 4 kDa. These peptides and, in addition, p16 (Fig. 1*G*) are also visible in SecA (*lane 2*) and N68 (*lane 5*) digests. Interestingly, upon trypsinolysis of all three polypeptides in the presence of 3K7L, p12 and p4 amounts generated are reduced or disappear completely, while a new fragment (p8) becomes prominent (Fig. 1, *lanes 3*, *6*, and *9*). Amino-terminal sequencing of p12, p4, and p8 generated from N1–349 (Fig. 4*B*; see "Experimental Procedures") revealed that p12 spans residues 220–329 (see Fig. 1*G*),

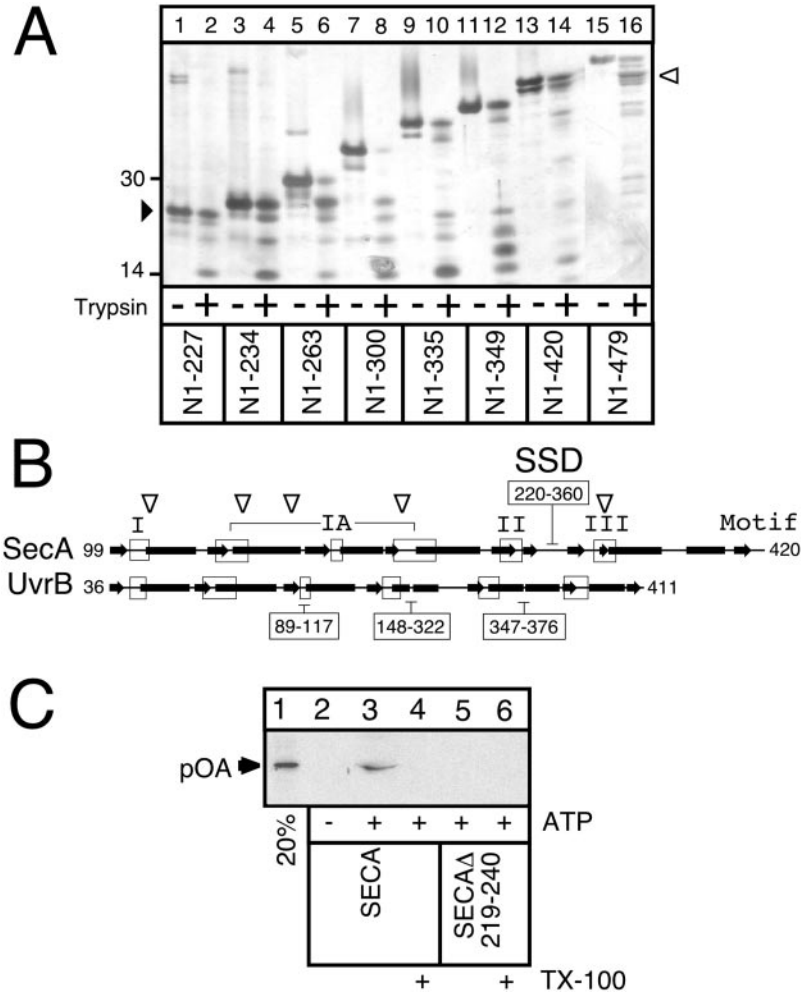

FIG. 3. **Structural features of the amino-terminal N ATPase region of SecA.** *A*, limited trypsinolysis of N68 truncations. N-domain fragments (27 μg in 30 μl of buffer B) were digested with trypsin (25 μg/ml; 3.5 min; 4 °C). The reaction was stopped with pefabloc (1 mM). An aliquot (6.5 μg) was analyzed by SDS-PAGE (10% hT gels) and silver staining. Protease-resistant fragments ~1–227 (*filled arrow*) and ~1–420 (*open arrow*) are indicated. *B*, secondary structure alignment of the amino-terminal region of SecA (residues 99–420) with that of the corresponding domains from the atomic resolution structures of UvrB from *Bacillus caldotenax* (38) (Protein Data Bank codes 1D9X and 1D9Z). SecA secondary structure prediction was performed on the EMBL server (54). The superfamily 2 DEAD helicase motifs (*boxes*) of SecA are as follows: I, ^{105}GEGKT^{109}; Ia, ^{128}VVTVNDYLA^{136}/^{160}GMPA^{163}/^{177}GTNNEYGFDYLR^{188}; II, ^{207}LVDEVD^{212}; III, ^{371}TLASIT^{376}. *Black bars*, α-helices; *arrows*, β-sheets. Defective signal peptide suppressors (T111N, Y134S, E148K, N179Y, and A373V) (42, 43) are indicated *above* SecA (*open arrows*). *Boxed numbers above* SecA and *below* UvrB, sequences not present in other DEAD proteins. *C*, SSD is essential for protein translocation. *In vitro* preprotein translocation in SecYEG-proteoliposomes of SecA and SecA-Δ219–240 as in Karamanou *et al.* (17). *Lane 1*, 50% of input [^{35}S]proOmpA. Triton X-100 (1% v/v) was added prior to trypsin digestion (*lanes 4* and *6*). Proteoliposomes are devoid of leader peptidase and do not result in signal peptide cleavage (53).

p4 is a collection of four peptides (p4.1–p4.4) that span the 124–200 region between DEAD motifs I and II, and p8 comprises two peptides (p8.1 and p8.2) within SSD that share sequences with p12.

To further examine signal peptide-induced conformational changes within SSD, we developed an independent, noninvasive assay that made use of monospecific polyclonal antibodies recognizing residues 244–385 of SSD (see "Experimental Procedures"). Preincubation of SecA (*lanes 1–3*) or N68 (*lanes 4–6*) with the 3K7L signal peptide causes significant reduction (30–35%) to the binding of the α-SSD antibody to SecA or N68 (Fig. 4*C*, *lanes 3* and *6*). A similar but less drastic effect is seen with an α-SecA antibody (*lanes 2* and *5*), whereas binding of α-C34 to SecA (*lane 1*) and of control α-MBP to maltose-binding protein (*lane 7*) are unaffected.

We conclude that although binding of 3K7L occurs upstream of residue 234 (Fig. 2 and Table I), it results in extensive conformational changes to N1–420. These cover extensive regions of NBD and SSD. Furthermore, differentially exposed tryptic cleavage sites may reveal residues directly involved in signal peptide binding.

Signal Peptide Binding at a Site Distinct from the ATP Binding Site Inhibits the ATPase of the DEAD Motor—Do signal peptide-induced conformational changes affect DEAD motor catalysis? To test this possibility, we examined the effect of 3K7L on ATP hydrolysis by N68 and derivatives (Fig. 5). At concentrations below 1 μM, 3K7L marginally stimulates the N-domain ATPase (Fig. 5*A*). However, at higher concentrations, 3K7L, but not nonfunctional signal peptide (1K2L; Ref. 24), reduces N68 ATPase significantly (Fig. 5, *A* and *B*). Similarly, 3K7L binding to N1–263 (Fig. 3, *C* and *D*; Table I) inhibits its ATPase activity (Ref. 18; Fig. 3*A*, *right*). We have no evidence that ATPase inhibition correlates with signal peptide-induced aggregation.[1]

This observation provided us with an enzymatic assay to test whether signal peptide binding takes place at ATPase catalytic motifs I and II (Figs. 2*A* and 3*B*). A range of 3K7L concentrations was added to N68 in the presence of increasing ATP concentrations. Linear transformation (Fig. 5*C*) of velocity curves (Fig. 3*B*) revealed that, while the K_m remained largely unaltered, turnover is repressed by at least 20-fold (43 min^{-1} in the absence *versus* 2 min^{-1} in the presence of 20 μM 3K7L), bringing N68 ATPase to the level of SecA (18). The inhibition constant (K_i) is 2.5 μM and is, as expected, similar to the determined binding constant for signal peptide (Table I). We conclude that 3K7L is a noncompetitive inhibitor of ATP hydrolysis, and it therefore binds to an allosteric site distinct from that of the nucleotide.

Signal Peptide Binding Affinity for the DEAD Motor Is Reduced by IRA1—In contrast to the effect on N68, the signal peptide-induced conformational changes effected on SecA (Fig. 4) do not alter its basal ATPase activity (Figs. 1*A* and 6*A*, *lanes 1* and *4*) (24). Furthermore, 3K7L binding to N68 is measurably higher (Figs. 1*C* and 2, *C* and *D*; Table I) than to SecA. Signal peptide binding to the DEAD motor may be under the control of the C-terminal IRA1 switch that represses ATP hydrolysis in soluble SecA (17, 18). To test this, we employed mutants with

[1] C. Baud, S. Karamanou, and A. Economou, unpublished observations.

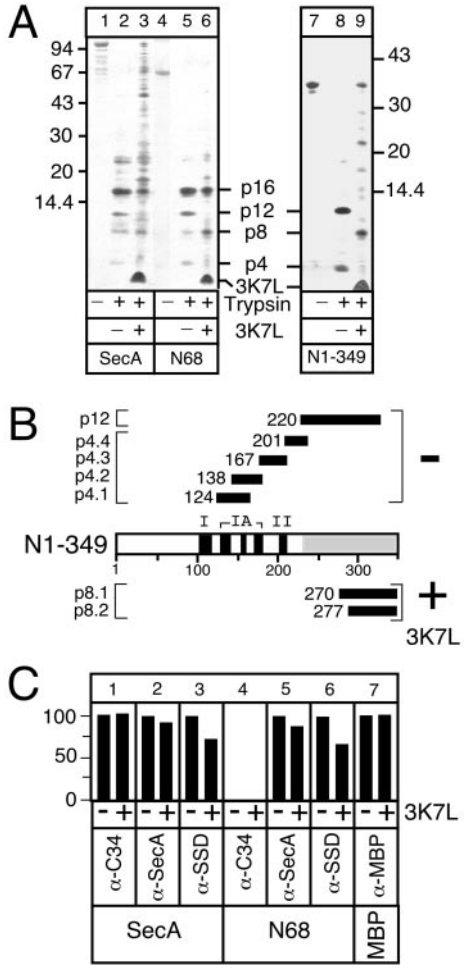

FIG. 4. **Binding of 3K7L induces conformational changes to the N1–420 domain.** *A*, proteins (20 μg) were digested with trypsin (25 μg/ml) for 45 min on ice, in the presence or absence of 10-fold molar excess of 3K7L. Samples (6.5 μg of each proteins) were analyzed by electrophoresis (10% hT gels) and silver staining. Molecular masses of markers (kDa) are indicated. *B*, map of N1–349 tryptic peptides. N-terminal residues (determined by Edman degradation) and C-terminal residues (estimated from the MW_{app} on 10% hT gels) are indicated: p12 (^{220}TPLI . . . IVK^{329}), p4.1 (^{124}GVHVV . . . PAK^{166}); p4.2 (^{138}DAENN . . . AKR^{167}); p4.3 (^{168}EYAAD . . . QRK^{202}); p4.4 (^{201}KLHYA . . . MYK^{237}); p8.1 (^{270}QVNL . . . TGR^{342}), p8.2 (^{277}GLVLI . . . TGR^{342}). The *shaded area* represents the 230–360 sequence. *C*, 3K7L affects antibody binding to SecA and N68. Proteins (150 pmol) were incubated (5 min; 20-μl reactions in buffer B) with a 3-fold molar excess of 3K7L (10 μg in 2 μl of Me_2SO; marked with a *plus sign*) or with 2 μl of Me_2SO; marked with a *minus sign*). Aliquots (2 μl) were spotted onto nitrocellulose using a vacuum manifold. Membranes were air-dried and incubated with indicated primary antisera followed by a horseradish peroxidase-coupled secondary antibody and visualized by chemiluminescence. Signals were quantitated by scanning densitometry. *MBP*, maltose-binding protein, used as a control.

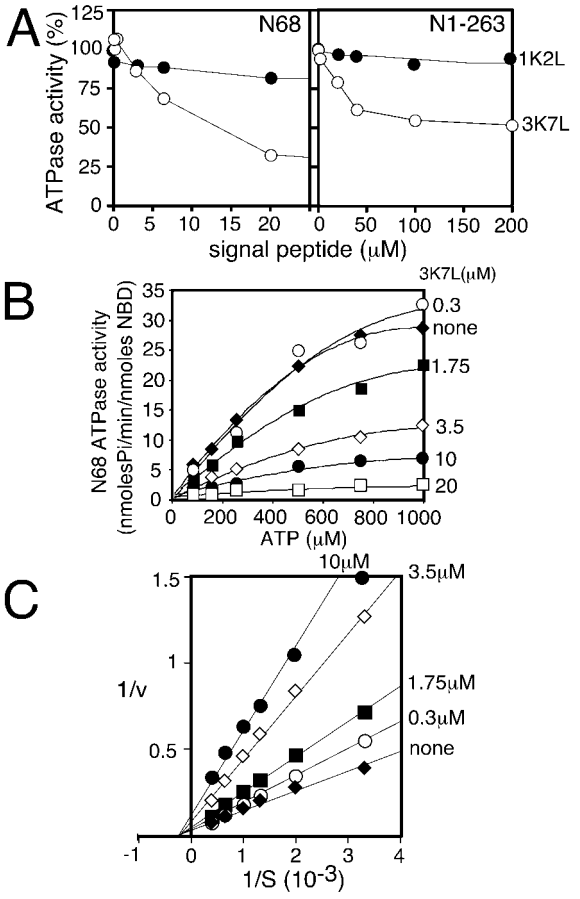

FIG. 5. **Signal peptide inhibits the ATPase activity of the N-domain.** *A*, N68 ATPase activity (as in Fig. 1*A*). N1–263 ATPase activity (100 pmol in buffer B; 1 mM [γ-^{32}P]ATP; 60 min; 37 °C) was quantitated by phosphorimaging of TLC plates (18). The effect of 3K7L on ATP hydrolysis was compared with that of the control signal peptide (1K2L). *B* and *C*, noncompetitive inhibition of N68 ATPase by signal peptide as shown by Lineweaver-Burke plots (*C*) of saturation kinetics (*B*). N68 (20 μg/ml), ATP (indicated amount), and 3K7L were incubated (30 min; 37 °C in buffer B), and released P_i was determined (as in *A*).

disabled IRA1 that mimic translocation-activated SecA: SecAΔIRA1 (missing residues 783–795) (17, 33) and SecAW775A (single tryptophanyl to alanyl substitution in IRA1).[2] Both mutants exhibit highly elevated basal ATPase activity (Fig. 6*A*, *lanes 2* and *3*) comparable with that of N68. In both cases, this elevated ATPase activity is suppressed by 3K7L (*lanes 5* and *6*).

Interestingly, cross-linking efficiency of [^{3}H]3K7L to SecAΔIRA1 and SecAW775A was increased by 2.4- and 2.7-fold, respectively, compared with that of SecA (Fig. 6*B*). Enhanced cross-linking is the result of a ~3-fold enhanced binding affinity of the two mutants to 3K7L as determined using the optical biosensor assay (Table I).

We conclude that signal peptide interaction with SecA is regulated by the IRA1 molecular switch. The signal peptide-mediated effects seen with N68 are not properties specific to the isolated DEAD motor domain but can also be detected with IRA1-mutated full-length SecA proteins.

DISCUSSION

We used a combination of biochemical and biophysical tools to identify the SecA signal peptide binding region and to probe the molecular basis of this interaction. Our data provide a cohesive molecular framework that links SecA structural elements to a functional interaction with preprotein and nucleotide ligands: (*a*) signal peptides bind to the ATPase N1–263 domain with high affinity; (*b*) binding occurs at a site that is distinct from both the catalytic ATPase determinants; (*c*) residues 227–263 in SSD, a novel substrate specificity domain, are essential for signal peptide binding; (*d*) binding of signal peptides causes conformational changes to the NBD and SSD regions of N1–420; (*e*) as a result, the ATPase activity of NBD is modulated; and (*f*) SecA/signal peptide interaction is controlled by the IRA1 switch.

This work extends and refines the dissection of SecA subdomains (17, 18) and reveals novel important features. Our results (Fig. 3, *A* and *B*) suggest that N1–420 is the largest

[2] E. Vrontou and A. Economou, unpublished results.

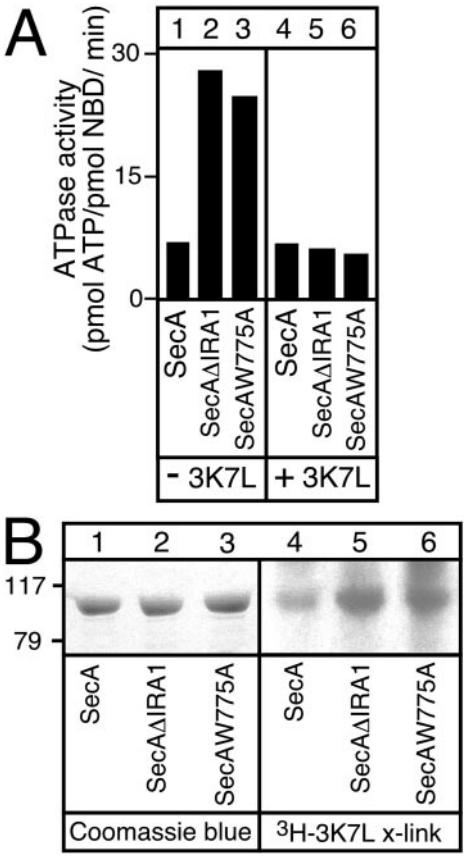

FIG. 6. **Signal peptide binding to SecA is controlled by the IRA1 switch.** *A*, ATP hydrolysis (as in Fig. 1*A*) by SecA and derivatives in the absence or presence of a 10-fold molar excess of signal peptide. *B*, SecA proteins (100 pmol in buffer H) were cross-linked with [^{3}H]3K7L and analyzed as in Fig. 1*C*.

discernible amino-terminal subdomain of the DEAD motor. N1–420 contains a minimal ATPase core that we have now delimited to the amino-terminal 1–227 residues (from the previous 1–263) (18). A novel N1–420 substructure (residues ~220–360; SSD) lies downstream of 1–227 and has inserted between DEAD motifs II and III (Fig. 3*B*). Three lines of evidence suggest that SSD is a structured domain that may be tightly integrated within N1–420 (Fig. 3): (*a*) a tryptic fragment containing most of SSD (p12) can be readily identified (Fig. 1); (*b*) SSD is more resistant to trypsinolysis when present in its full-length in C-terminally truncated N1–420 derivatives (Fig. 3); (*c*) secondary structure analysis predicts that SSD contains secondary structure and that it is extensively α-helical. Other DEAD motors are built from structurally homologous RecA-like nucleotide binding domains (21) from which dissimilar substrate specificity subdomains "sprout out" (*e.g.* UvrB; see Fig. 3*B*) (38–40) without affecting the overall RecA fold (21). We propose that SSD is one such domain allowing SecA to specifically recognize preprotein substrates. In agreement with this, SSD is essential for signal peptide binding (Fig. 2, Table I) and protein translocation (Fig. 3*C*), is implicated in full-length preprotein cross-linking (31), and contains Tyr-326 that is important for preprotein interaction (41).

Signal peptide binding activity is fully contained on N1–263 and to a large extent on N1–234 as revealed by cross-linking studies and surface plasmon resonance analysis (Fig. 2, *C* and *E*). This was further corroborated by the fact that the these fragments maintain binding affinities that are similar to those of SecA and N68 (Table I). Our experiments indicate that although the main elements of the binding pocket are present on N1–234 residues 234–263 are necessary to either optimize binding or to structurally stabilize the binding site proper. Interestingly, the removal of residues 227–234 reduces N1–227 affinity for signal peptides dramatically (Table I). This heptapeptide may be an essential component of the binding cleft. However, the alternative explanation that N1–227 has a localized structural defect undetectable by far UV CD cannot be ruled out. Partial deletion of SSD (SecAΔ219–240) abrogates signal peptide binding (Fig. 2, *C* and *E*). This result taken together with truncation analysis demonstrates unequivocally that residues 220–240 are essential for signal peptide binding. One possibility is that the 220–240 region is directly involved in signal peptide binding. However, since neither N1–227 (Fig. 2) nor p12 (220–329; Fig. 1*G*) nor SecAΔ219–240 measurably bind signal peptide, an alternative possibility is that the signal peptide binding site may be a composite of surfaces from both the NBD core (residues 1–227) and the 220–263 region of SSD. Such an organization could explain the effect of signal peptide binding on the accessibility of several residues in the 124–200 and 220–237 regions (Fig. 4, *A* and *B*) and would rationalize the widespread occurrence of suppressor mutations throughout the ATPase subdomain (Fig. 3*B*) (42, 43). Elucidation of these questions necessitates crystallographic studies (44). The only available structure of a signal peptide binding pocket is the M-domain of SRP54 (1).

Although high affinity signal peptide binding to SecA occurs at a site lying largely within N1–234 (Fig. 2, *C* and *E*, and Table I), conformational changes that result from binding are detectable within the downstream 270–340 region of SSD (Fig. 4). Although not essential for signal peptide binding (*e.g.* N1–263; Fig. 2, *B* and *C*), this region has been cross-linked to preproteins (31). Since defective peptides prevent preprotein cross-linking to SecA (45), signal peptide binding to the 1–234 region could allosterically promote the association of the mature preprotein segments with the SSD domain.

Signal peptide binding to SecA is regulated by the C-terminal IRA1 switch (Fig. 6), since the affinity constant (3.5 μM) is increased 3-fold in IRA1 SecA mutants and in N68 (Figs. 2 and 6; Table I). Binding of full-length preprotein-SecB complexes to translocase is of even higher affinity (0.06 μM) due to the separate affinities of SecA with the mature preprotein domain and with SecB (25, 46). The observed increase in binding affinity for the IRA1 mutants is concomitant with increase of SecA basal ATPase (Fig. 6*A*) (17). This exciting finding places interaction with both NBD ligands (preproteins and ATP) under common regulatory control. Interestingly, binding of signal peptide (27) or ATP (47) to SecA is sensed by tryptophanyl residue 775 within IRA1. IRA1 could operate as a safety latch ensuring that preprotein binding to cytoplasmic SecA will not activate the ATPase activity until the ternary complex reaches the membrane and binds productively to SecY. We anticipate that IRA1 mutants mimic the SecY-mediated activated state of SecA (17).

Through binding to the amino-terminal subdomain, signal peptides act as allosteric effectors of the DEAD motor ATPase (Fig. 5). Signal peptide-induced ATPase repression was also observed with chymotryptic N-terminal fragments of SecA (48). In agreement with these observations, the SecAY134C and SecAA373V signal suppressors have a slightly altered conformation and display elevated ATPase activity (49). Repression is not the result of enhanced ADP retention but rather stems from prevention of ATP hydrolysis.[3] In SecYEG-bound SecA, this would promote SecA membrane insertion (6), explaining why, unlike the nonhydrolyzable analogue AMP-PNP, ATP alone cannot drive SecA insertion but requires the preprotein

[3] S. Karamanou and A. Economou, unpublished results.

(7). The PrlA4 SecY mutant that can translocate signalless preproteins may stabilize the signal peptide-induced conformation of the SecA 1–420 domain (50). In agreement with this, signal peptides promote SecA insertion into model membranes (51), a reaction that is regulated by the amino-terminal region of SecA (52).

Taken together, our data and previous observations suggest an ordered cascade of events. (*a*) In cytoplasmic SecA, binding of the C-domain to the N-domain represses both ATP hydrolysis and preprotein binding. (*b*) SecA binding to SecY switches off IRA1-mediated suppression. (*c*) This enhances signal peptide binding to the SecA DEAD motor and causes localized conformational changes to both SSD and NBD. These changes could promote efficient binding of the preprotein mature domain (45)-SecB (25) complexes onto SecA and also facilitate ATP-driven SecA membrane insertion (6, 51). Quantitative, real time assays and purified SecA subdomains render predictions from the above model amenable to immediate testing.

Acknowledgments—We are grateful to M. Sioumpara (Krambovitis laboratory, Institute of Molecular Biology and Biotechnology) for peptide synthesis; A. Kuhn, K. Tokatlidis, D. Alexandraki, and D. Tzamarias for comments on the manuscript; A. Martinou, E. Gedig, and I. Tsigos for protocols; D. Oliver for plasmids; and C. Stassinopoulou, M. Pelekanou, and V. Bouriotis for use of equipment.

REFERENCES

1. Keenan, R. J., Freymann, D. M., Stroud, R. M., and Walter, P. (2001) *Annu. Rev. Biochem.* **70,** 755–775
2. Driessen, A. J. (2001) *Trends Microbiol.* **9,** 193–196
3. Johnson, A. E., and van Waes, M. A. (1999) *Annu. Rev. Cell Dev. Biol.* **15,** 799–842
4. Economou, A. (2000) *FEBS Lett.* **476,** 18–21
5. Driessen, A. J., Manting, E. H.,. and van der Does, C. (2001) *Nat. Struct. Biol.* **8,** 492–498
6. Economou, A., and Wickner, W. (1994) *Cell* **78,** 835–843
7. Economou, A., Pogliano, J. P., Beckwith, J., Oliver, D. B., and Wickner, W. (1995) *Cell* **83,** 1171–1181
8. Economou, A. (1998) *Mol. Microbiol.* **27,** 511–518
9. Schiebel, E., Driessen, A. J. M., Hartl, F.-U., and Wickner, W. (1991) *Cell* **64,** 927–939
10. van der Wolk, J. P., de Wit, J. G., and Driessen, A. J. (1997) *EMBO J.* **16,** 7297–7304
11. Joly, J. C., and Wickner, W. (1993) *EMBO J.* **12,** 255–263
12. Meyer, T. H., Menetret, J. F., Breitling, R., Miller, K. R., Akey, C. W., and Rapoport, T. A. (1999) *J. Mol. Biol.* **285,** 1789–1800
13. Manting, E. H., van Der Does, C., Remigy, H., Engel, A., and Driessen, A. J. (2000) *EMBO J.* **19,** 852–861
14. Nishiyama, K., Fukuda, A., Morita, K., and Tokuda, H. (1999) *EMBO J.* **18,** 1049–1058
15. Nishiyama, K., Suzuki, T., and Tokuda, H. (1996) *Cell* **85,** 71–81
16. Duong, F., and Wickner, W. (1997) *EMBO J.* **16,** 4871–4879
17. Karamanou, S., Vrontou, E., Sianidis, G., Baud, C., Roos, T., Kuhn, A., Politou, A., and Economou, A. (1999) *Mol. Microbiol.* **34,** 1133–1145
18. Sianidis, G., Karamanou, S., Vrontou, E., Boulias, K., Repanas, K., Kyrpides, N., Politou, A. S., and Economou, A. (2001) *EMBO J.* **20,** 961–970
19. Koonin, E. V., and Gorbalenya, A. E. (1992) *FEBS Lett.* **298,** 6–8
20. Hirano, M., Matsuyama, S., and Tokuda, H. (1996) *Biochem. Biophys. Res. Commun.* **229,** 90–95
21. Bird, L. E., Subramanya, H. S., and Wigley, D. B. (1998) *Curr. Opin. Struct. Biol.* **8,** 14–18
22. Hall, M. C., and Matson, S. W. (1999) *Mol. Microbiol.* **34,** 867–877
23. Shinkai, A., Mei, L. H., Tokuda, H., and Mizushima, S. (1991) *J. Biol. Chem.* **266,** 5827–5833
24. Miller, A., Wang, L., and Kendall, D. A. (1998) *J. Biol. Chem.* **273,** 11409–11412
25. Fekkes, P., de Wit, J. G., van der Wolk, J. P., Kimsey, H. H., Kumamoto, C. A., and Driessen, A. J. (1998) *Mol. Microbiol.* **29,** 1179–1190
26. Wang, L., Miller, A., and Kendall, D. A. (2000) *J. Biol. Chem.* **275,** 10154–10159
27. Ding, H., Mukerji, I., and Oliver, D. (2001) *Biochemistry* **40,** 1835–1843
28. Roos, T., Kiefer, D., Hugenschmidt, S., Economou, A., and Kuhn, A. (2001) *J. Biol. Chem.* **276,** 37909–37915
29. Lill, R., Dowhan, W., and Wickner, W. (1990) *Cell* **60,** 271–280
30. van Voorst, F., Vereyken, I. J., and de Kruijff, B. (2000) *FEBS Lett.* **486,** 57–62
31. Kimura, E., Akita, M., Matsuyama, S., and Mizushima, S. (1991) *J. Biol. Chem.* **206,** 6600–6606
32. Mitchell, C., and Oliver, D. (1993) *Mol. Microbiol.* **10,** 483–497
33. Jarosik, G. P., and Oliver, D. B. (1991) *J. Bacteriol.* **173,** 860–868
34. Schagger, H., and von Jagow, G. (1987) *Biochemistry* **166,** 368–379
35. Izard, J. W., Doughty, M. B., and Kendall, D. A. (1995) *Biochemistry* **34,** 9904–9912
36. Seligman, S. J. (1993) *Anal. Biochem.* **211,** 324–325
37. O'Shannessy, D. J., Brigham-Burke, M., Soneson, K. K., Hensley, P., and Brooks, I. (1993) *Anal. Biochem.* **212,** 457–468
38. Theis, K., Chen, P. J., Skorvaga, M., Van Houten, B., and Kisker, C. (1999) *EMBO J.* **18,** 6899–6907
39. Moolenaar, G. F., Höglund, L., and Goosen, N. (2001) *EMBO J.* **20,** 6140–6149
40. Machius, M., Henry, L., Palnitkar, M., and Deisenhofer, J. (1999) *Proc. Natl. Acad. Sci. U. S. A.* **96,** 11717–11722
41. Kourtz, L., and Oliver, D. (2000) *Mol. Microbiol.* **37,** 1342–1356
42. Fikes, J. D., and Bassford, P. J., Jr. (1989) *J. Bacteriol.* **171,** 402–409
43. Huie, J. L., and Silhavy, T. J. (1995) *J. Bacteriol.* **177,** 3518–3526
44. Weinkauf, S., Hunt, J. F., Scheuring, J., Henry, L., Fak, J. Oliver, D. B., and Deisenhofer, J. (2001) *Acta Crystallogr. D Biol.* **57,** 559–565
45. Akita, M., Sasaki, S., Matsuyama, S., and Mizushima, S. (1990) *J. Biol. Chem.* **265,** 8164–8169
46. Hartl, F.-U., Lecker, S., Schiebel, E., Hendrick, J. P., and Wickner, W. (1990) *Cell* **63,** 269–279
47. den Blaauwen, T., Fekkes, P., de Wit, J. G., Kuiper, W., and Driessen, A. J. M. (1996) *Biochemistry* **35,** 11194–12004
48. Triplett, T. L., Sgrignoli, A. R., Gao, F. B., Yang, Y. B., Tai, P. C., and Gierasch, L. M. (2001) *J. Biol. Chem.* **276,** 19648–19655
49. Schmidt, M., Ding, H., Ramamurthy, V., Mukerji, I., and Oliver, D. (2000) *J. Biol. Chem.* **275,** 15440–15448
50. Derman, A. I., Puziss, J. W., Bassford, P. J., Jr., and Beckwith, J. (1993) *EMBO J.* **12,** 879–888
51. Ahn, T., and Kim, H. (1996) *J. Biol. Chem.* **271,** 12372–12379
52. McNicholas, P., Rajapandi, T., and Oliver, D. (1995) *J Bacteriol.* **177,** 7231–7237
53. Brundage, L., Hendrick, J. P., Schiebel, E., Driessen, A. J., and Wickner, W. (1990) *Cell* **62,** 649–657
54. Rost, B., and Sander, C. (1995) *Proteins* **23,** 295–300